Organic & Biomolecular Chemistry

Accepted Manuscript

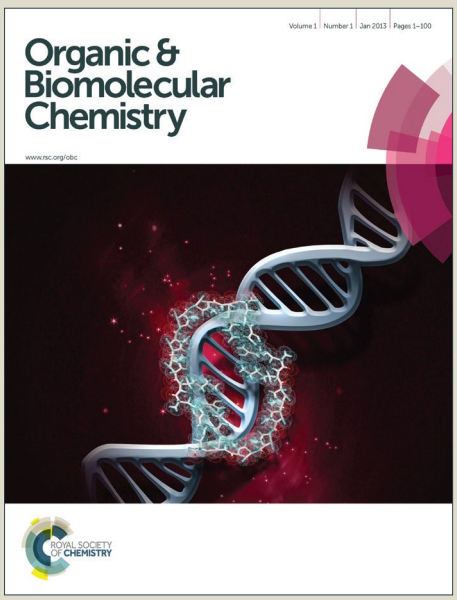

ROYAL SOCIETY OF CHEMISTRY

www.rsc.org/obc

Design of a Fluorescent Ligand Targeting the S-adenosylmethioine Binding Site of the Histone Methyltransferase MLL1

Yepeng Luan[1†], *Levi L. Blazer*[2†], *Hao Hu*[1], *Taraneh Hajian*[2], *Jing Zhang*[1], *Hong Wu*[2], *Scott Houliston*[2] *and Cheryl H. Arrowsmith*[2,3], *Masoud Vedadi*[2,4]*, *Yujun George Zheng*[1]*

[1]Department of Pharmaceutical and Biomedical Sciences, University of Georgia, Athens, Georgia 30602, United States.

[2]Structural Genomics Consortium, University of Toronto, Toronto, Ontario, M5G 1L7, Canada

[3]Princess Margaret Cancer Centre and Department of Medical Biophysics, University of Toronto, Toronto, ON, M5G 2M9.

[4]Department of Pharmacology and Toxicology, University of Toronto, Toronto, ON, M5S 1A8.

* To whom correspondence should be addressed:

Y. G. Zheng; Tel: (706) 542-0277; Fax: (706) 542-5358; E.mail: yzheng@uga.edu

M. Vedadi; Tel: (416) 432-1980; E.mail: m.vedadi@utoronto.ca

†equal contributions

Keywords: Methyltransferase, MLL1, SAM analog, fluorescent probe

ABSTRACT

The histone methyltransferase MLL1 has been linked to translocation-associated gene fusion in childhood leukemias and is an attractive drug target. High-throughput biochemical analysis of MLL1 methyltransferase activity requires the production of at least a trimeric complex of MLL1, RbBP5 and WDR5 to elicit robust activity. Production of trimeric and higher order MLL1 complexes in the quantities and reproducibility required for high-throughput screening presents a significant impediment to MLL1 drug discovery efforts. We present here a small molecule fluorescent ligand (FL-NAH, **6**) that is able to bind to the *S*-adenosylmethionine (SAM) binding site of MLL1 in a manner independent of the associated complex members. We have used FL-NAH to develop a fluorescence polarization-based SAM displacement assay in a 384-well format targeting the MLL1 SET domain in the absence of associated complex members. FL-NAH competes with SAM and is displaced from the MLL1 SET domain by other SAM-binding site ligands with K_{disp} values similar to the higher-order complexes, but is unaffected by the H3 peptide substrate. This assay enables screening for SAM-competitive MLL1 inhibitors without requiring the use of trimeric or higher order MLL1 complexes, significantly reducing screening time and cost.

INTRODUCTION

The SET1 family of lysine methyltransferases is comprised of six members in mammals (SET1A, SET1B, and MLL1-4) that perform the majority of H3K4 mono-, di-, and trimethylation *in vivo*[1-3]. SET1 family members require at least two accessory proteins (WDR5 and RbBP5) for efficient methyltransferase activity[4-7]. Formation of higher-order complexes by the sequential addition of ASH2L and DPY-30 further enhance the enzymatic competency of these proteins[6]. Due to its pronounced oncogenic potential, MLL1 (mixed-lineage leukemia 1) has become one of the most thoroughly characterized members of the SET1 family. MLL1 facilitates transcription by increasing H3K4 methylation at the promoters, transcriptional start sites, and 5' transcribed regions of actively transcribed genes[8]. This stimulatory activity is essential for development and expansion of the hematopoietic system by regulating the expression of *Meis* and *Hox* cluster genes[1, 6, 8].

MLL1 dysregulation has been strongly linked to a variety of human malignancies; indeed, MLL1-rearrangements has been detected in approximately 5% of acute lymphoblastic leukemias (ALL) and 5-10% of acute myeloid leukemia (AML) cases in adults as well as in more than 70% of infant ALL and 35-50% of infant AML patients (reviewed by Chen and Armstrong)[9]. These translocations generate a fusion protein of the N-terminal region of MLL1 with one of several transcriptional elongators, including AF4, AF9, ENL, and ELL[9, 10]. The oncogenic potential of these fusion proteins stem from the recruitment of the fusion protein to the super elongation complex leading to dysregulated expression of normal MLL targets, including *MEIS1* and the *Hox* cluster genes[8-10].

Several attempts to inhibit the function of MLL fusion proteins with small molecules have been reported in the literature[11-15]. However, a wild-type allele of MLL1 is required for the

transformative capacity of the oncogenic fusion proteins[16], leading us and others to target the catalytic activity of wild-type MLL1[17, 18]. Significant progress has been made in both of these areas, including targeting the MLL-menin and MLL-WDR5 interactions[11-15, 17-19]. Recently OICR-9429, a WDR5 antagonist has been reported to dissociate the MLL1-WDR5-RbBP5 complex, selectively inhibit proliferation, and induce differentiation in p30-expressing human AML cells[20]. To date, no compounds that directly target the SAM- or substrate-binding sites of the MLL1 SET domain have been reported.

While methods for generating SET1 family complexes have been established in our lab, it is rather time consuming and costly to produce the quantities of high-quality protein complex needed to perform high-throughput screening (HTS). Keeping the MLL1 complex fully stable and active for duration of the screening experiments may also be challenging. To this end, we have developed a simple, HTS-amenable assay that does not require generation of high-order MLL1 complexes. This assay is based upon a small molecule fluorescent ligand that specifically binds to the SAM-binding site of the MLL1 SET domain. This ligand binds in a similar manner to the isolated MLL1 SET domain as it does to higher order MLL1 complexes and is displaced by SAM analogs with similar K_{disp} values in the isolated MLL1 domain and the higher-order complexes. This compound represents a valuable tool to the development of SAM-binding site-specific inhibitors of MLL1.

RESULTS AND DISCUSSION

Design and synthesis of FL-NAH.

The histone methyltransferase MLL1 is involved in translocation-associated gene fusion in childhood leukemia and is a promising drug target. Biochemical screening for MLL1 inhibitors typically requires the production of at least a trimeric complex of MLL1, RbBP5 and

WDR5 to elicit robust activity. Production of trimeric and higher order MLL1 complexes in the quantities and reproducibility required for high-throughput screening presents a significant challenge to MLL1 drug discovery efforts. Therefore, we have developed a fluorescent ligand that binds to the SAM-binding site of MLL1. We have used this ligand to develop a miniaturized biochemical assay to identify and characterize MLL1 SET-domain inhibitors.

The fluorescent ligand (fluorescein linked with Aza-adenosylhomocysteine, FL-NAH) is built based on the backbone structure of the AdoMet cofactor (**Figure 1**). It contains a fluorescein fluorophore linked to the cofactor mimetic Aza-adenosylhomocysteine (NAH) via a triazole linker. NAH possesses all the essential binding elements (e.g. electrostatic, H-bonds, and π—π stacking) of the native cofactor required for strong interaction with the active site of MLL1. We envisaged that the rigid triazole linker could also contribute to the ligand interaction with the enzyme. Previously, fluorescently labeled AdoMet analogs have been made with a fluorophore attached to the N6 position of the adenyl ring or the ribose hydroxyls[21-23]. However, there are no reports that describe ligands with a fluorophore tethered to the junction between the adenosyl and the 2-aminobutanoate moieties of Aza-adenosylhomocysteine.

The synthetic route is shown in Scheme 1. Compound **1** was obtained with high yield by condensation between the commercially available 5-FAM and the 2-azido-ethanamine with the coupling reagents HOBt and EDCI in anhydrous DCM. The synthesis of compound **2** to **5** started from 2′,3′-*O*-isopropylideneadenosine and followed the modified procedures reported in the literature[24, 25]. The sequential azidation and reduction of 2′,3′-*O*-isopropylideneadenosine yielded compound **3**. Then compound **3** was condensed with *tert*-butyl (*S*)-2-((*tert*-butoxycarbonyl)amino)-4-oxobutanoate under reductive environment to give the intermediate compound **4** which was then alkylated with propargyl bromide to afford compound **5**. The final

click reaction was performed with the regular catalyst of copper (II) sulfate and sodium ascorbate in the mixture of methanol and ddH_2O to yield the final product FL-NAH (**6**).

Measurement of MLL1-FL-NAH binding affinity: FL-NAH bound in a saturable manner to the SET domain of MLL1 in the context of the enzymatically active trimeric, tetrameric, and pentameric complexes as well as in the absence of these accessory proteins (**Figure 2, Supplementary Figure 1, Table 1**). In all cases the maximal FP shift observed with saturating concentrations of protein was similar. FL-NAH bound the isolated MLL1 SET domain with an affinity similar to that of the enzymatically competent complexes, suggesting that the SET domain of MLL1 possesses a structured SAM-binding site even in the absence of associated complex members (**Figure 2**, **Table 1**). This is consistent with the crystal structure of the isolated MLL1 SET domain[26] (PDB ID: 2W5Y), where the SAM-binding site is well-ordered in the absence of the associated complex members. Furthermore, increased catalytic efficiency observed in the presence of higher-order MLL1 complexes can be explained by a rearrangement of the I-SET domain that orients the substrate lysine side chain in a more stable conformation, suggesting that increased affinity for SAM is not necessarily a requisite component of the higher-order MLL1 complexes[26]. Binding of FL-NAH to MLL1 SET domain alone was also confirmed by saturation-transfer difference (STD) NMR (**Supplementary Figure 2**) and differential static light scattering (**Supplementary Figure 3**).

FL-NAH displacement by SAM-binding site ligands: To confirm that FL-NAH binds specifically to the SAM-binding site of MLL1, we tested the ability of several known SAM-binding site ligands to displace FL-NAH. MLL1 complexes and isolated SET domain were

diluted to their respective K_d concentrations and incubated with 50 nM FL-NAH in the presence of increasing concentrations of SAM, the reaction product SAH, or the fungal SAM-binding site inhibitor sinefungin (**Figure 3A, 3B, 3C, Table 2**) and the K_{disp} was determined by fitting the data to Eq. (2) using non-linear least squares regression in GraphPad Prism v.6.05. A peptide corresponding to residues 1 to 25 of histone H3 (MLL1 substrate) was used as a control which did not displace FL-NAH (**Figure 3D**). The reaction product SAH is a particularly well-suited inhibitor for *in vitro* analysis of SAM-dependent methyltransferases. Indeed, in this assay format, SAH displaces FL-NAH from the isolated SET domain of MLL1 with a K_{disp} of 4 ± 0.5 μM (**Figure 3B, Table 2**). The potency of FL-NAH displacement by SAH increases as more complex members are added to the MLL SET domain, resulting in a 20-fold increase in potency for the pentameric complex relative to the isolated SET domain. Similar increases in potency were observed for SAM and sinefungin, suggesting that this is a general effect for this protein complex. This increase in potency presumably stems from a better packing of SAM-binding site in the higher order complexes leading towards higher affinity for SAM and its analogues.

Amenability of the assay to screening in a 384-well format: The isolated SET domain was used to develop a miniaturized FP binding assay. The K_d concentration of MLL1 isolated SET domain (1 μM) was chosen to balance assay signal-to-noise ratio with the sensitivity of the assay to detect inhibitors. The assay was miniaturized to a 384-well format in a total volume of 10 μl and formatted in a mix-and-read manner comprising two additions to the well; the first addition being a solution containing MLL1 and FL-NAH, the second being the addition of the test compound or appropriate control. In this format, the assay is stable for several hours at ambient temperature (~23ºC, data not shown) and is insensitive to the concentrations of DMSO (**Figure**

4A) that are essential for compound screening. The assay is robust and amenable to HTS, routinely providing Z' values of ≥0.7 when a saturating concentration of SAH is used as a positive control (**Figure 4B**).

CONCLUSION

We have described the synthesis and characterization of FL-NAH, a SAM-binding site probe for MLL1 that does not require accessory complex members. We have used FL-NAH to develop an FP-based screening assay that will facilitate efficient high-throughput screening for the discovery of MLL1 SAM-binding site ligands without the need for the production of multi-protein complexes. This assay is robust and is inhibited by known SAM-binding site ligands with K_{disp} values that are similar to the higher-order complexes currently being used for chemical biology studies. While compounds discovered using this assay format will require follow-up studies using more physiologically relevant MLL1 complexes, it provides a simple method by which one can quickly screen large compound libraries for SAM-binding site ligands of the MLL1 SET domain.

MATERIALS AND METHODS

Reagents and general procedures.

5-Carboxyfluorescein (5-FAM) was purchased from ChemPep Inc. with high purity. All other starting materials were purchased from Sigma-Aldrich. The solvent for chemical synthesis and column chromatography purification were all analytical grade. The intermediates (compound **1** to **5**) were purified by silica gel (200-300 mesh) column chromatography. The final product (compound **6**) was purified by preparative HPLC (YMC Pack Pro C18 AS12S05-1520WT, 120

Å, 5 μm, 150 × 20 mm) with water (HPLC grade, +0.1% TFA) (A) and acetonitrile (HPLC grade, +0.1% TFA) (B) under 214 nm and 260 nm using gradient elution (B% from 5% to 60%, 0 min to 51min, 4 mL/min). The structures of all intermediates and final product were confirmed by mass spectrum and NMR. The purity of the final product was analyzed by analytical HPLC (Waters Nova-Park C18, 60 Å, 4 μm 150 × 3.9 mm column, 1 mL/min, under 214nm, B%=30% for 33min). The spectral data of compound **1-5** in this manuscript are consistent with the literature reports.[24, 25, 27]

Synthesis procedures and compound characterization.

*5-(2'-azidoethylamino)carbonylfluorescein (**1**)*[27]. A mixture of 5-FAM (51.6 mg, 0.137 mmol, 1.0 eq.), Hydroxybenzotriazole (HOBt, 26 mg, 0.192 mmol, 1.5 eq.) and 1-Ethyl-3-(3-dimethylaminopropyl)carbodiimide (EDCI, 36.8 mg, 0.192 mmol, 1.5 eq.) was dissolved in 5 mL anhydrous DMF under nitrogen protection. DIPEA (133 μL, 0.768 mmol, 3.0 eq.) was injected to the reaction solution. The reaction mixture was stirred at room temperature for 1h. Then, the 2-azido-ethylamine 32.3 mg, 0.376 mmol, 1.5 eq.) dissolved in 500 μL anhydrous DMF was injected to the mixture. The reaction was continued for 24 h at room temperature in the darkness. The DMF was evaporated and the crude product was purified by column chromatography (DCM:MeOH = 10:1) to give pure compound **1** as a yellow powder (18 mg, 35%). H^+ESI = 445.1. ^{1}H-NMR (400 MHz, methanol-D_4) δ = 3.55 (t, 2H, *J* = 5.76 Hz), 3.64 (t, 2H, *J* = 5.76 Hz), 6.69 (d, 2H, *J* = 8.40Hz), 6.79-6.84 (m, 4H), 7.38 (d, 1H, *J* = 8.00 Hz), 8.23 (dd, 1H, *J*1 = 8.04 Hz, *J*2 = 1.04 Hz), 8.53 (s, 1H).

*9-((3aR,4R,6R,6aR)-6-Azidomethyl-2,2-dimethyl-tetrahydro-furo[3,4-d]-1,3-dioxol-4-yl)-9H-purin-6-ylamine (**2**)*[24, 25]. To 3.25 mmol of 2',3'-O-isopropylideneadenosine (1.00 g, 1.0 eq., 3.25

mmol) suspended in anhydrous 1,4 dioxane (10 mL) was added 6.51 mmol of diphenylphosphoryl azide (DPPA, 1.40 mL, 2.00 eq., 6.51 mmol) and 9.77 mmol of DBU (1.46 mL, 3.00 eq., 9.77 mmol) at room temperature under N_2. The solution was stirred for 16 hours after which 32.5 mmol of NaN_3 (2.11 g, 10 eq.) and 65 µmol of 15-crown-5 (0.1 eq.) were added and the reaction mixture was heated to reflux. After 4 hours the solid was removed by filtration. The solvent was evaporated and the crude product was purified by column chromatography (ethyl acetate/petroleum ether 1:1, to ethanol/ethyl acetate 1:5, silica). After drying under high vacuum, a colorless solid (compound **2**) was obtained (1.08 g, 100%). H^+ESI = 333.1. ^{1}H-NMR (400MHz, $CDCl_3$) δ = 1.38 (s, 3H), 1.60 (s, 3H), 3.57 (m, 2H), 4.37 (m, 1H), 5.05 (dd, 1H, *J*1 = 5.08 Hz, *J*2 = 2.72 Hz), 5.45 (dd, 1H, *J*1 = 5.12 Hz, *J*2 = 1.72 Hz), 6.10 (d, 1H, *J* = 1.76 Hz), 6.28 (s, 2H), 7.91 (s, 1H), 8.33 (s, 1H).

*9-((3aR,4R,6R,6aR)-6-Aminomethyl-2,2-dimethyl-tetrahydro-furo[3,4-d]-1,3-dioxol-4-yl)-9H-purin-6-ylamine (**3**)*[24, 25]. 74 mg compound **2** was dissolved in 10 mL methanol, then 25 mg Pd/C was added. The mixture was stirred in hydrogen atmosphere at room temperature for 2.5 h. After filtering off the Pd/C, the solvent was removed by evaporation and the residue was dried under vacuum to give a white solid (60 mg, 88%). H^+ESI = 307.2. ^{1}H-NMR (400MHz, CD_3OD) δ = 1.36 (s, 3H), 1.58 (s, 3H), 2.86-2.90 (m, 2H), 4.24-4.18 (m, 1H), 5.00 (dd, 1H, *J*1 = 6.80 Hz, *J*2 = 3.60 Hz), 5.46 (dd, 1H, *J*1 = 6.40 Hz, *J*2 = 3.20 Hz), 6.13 (d, 1H, *J* = 2.80 Hz), 8.20 (s, 1H), 8.26 (s, 1H).

5′-N-[4-{(2S)-2-(N-tert-Butoxycarbonyl)amino-butyric acid}

*]tert-butyl ester-5′-deoxy-2′,3′-O,O-(1-methyl ethylidene) adenosine (**4**)*[24, 25]. Compound **3** (0.544 g, 1.78 mmol, 1.0 eq.) was dissolved in 10 mL anhydrous dichloroethene (DCE). Under stirring, the *tert*-butyl (*S*)-2-((*tert*-butoxycarbonyl)amino)-4-oxobutanoate (0.46 g, 1.7 mmol, 1.0

eq.) was added in one portion followed by the sodium triacetoxyborohydride (0.38 g, 1.78 mmol, 1 eq.). The mixture was stirred at room temperature for 3 h. Saturated aqueous sodium bicarbonate (20 mL) was added to the mixture then was extracted by dichloromethane (DCM, 5 mL×3). The organic layer was collected, washed with brine and dried over Na_2SO_4. After removal of the solvent, the crude product was purified by column chromatography to give pure compound **4** as a white solid (0.762 g, 76%). H^+ESI = 564.3. ^{1}H-NMR (400MHz, $CDCl_3$) δ = 1.35 (s, 9H), 1.36 (s, 3H), 1.43 (s, 9H), 1.60 (s, 3H), 1.84 (m, 1H), 2.36 (m, 1H), 3.04 (m, 1H), 3.14 (m, 1H), 3.40 (m, 2H), 4.18 (s, 1H), 4.54 (d, 1H, *J* = 3.64 Hz), 5.08 (s, 1H), 5.25 (d, 1H, *J* = 5.20 Hz), 5.55 (d, 1H, *J* = 5.20 Hz), 6.20 (s, 1H), 8.28 (s, 1H), 8.30 (s, 1H).

*5′-N-propynylamino-N′-[4-{(2S)-2-(N-tert-butoxycarbonyl)amino-butyric acid}] tert-butyl ester-5′-deoxy- 2′,3′-O,O-(1-methylethylidene)adenosine (**5**)*[24, 25]. Compound **4** (78 mg, 0.15 mmol, 1.0 eq.) was dissolved in anhydrous DMF (5 mL). Under stirring, propargyl bromide (18.2 mg, 0.15 mmol, 1.2 eq.) was added followed by K_2CO_3 (21 mg, 0.15 mmol, 1 eq.). The reaction mixture was stirred at room temperature for 24h. Water was added and the mixture was extracted by DCM (x3). The organic layer was collected and dried over Na_2SO_4. The crude product was purified by column chromatography to give pure compound **5 (**67 mg**,** 75%**).** H^+ESI = 602.3. ^{1}H-NMR (400MHz, $CDCl_3$) δ = 1.37 (s, 3H), 1.41 (s, 9H), 1.43 (s, 9H), 1.60 (s, 3H), 1.91 (m, 1H), 2.17 (m, 1H), 2.46 (s, 1H), 3.11 (m, 2H), 3.36-3.46 (m, 2H), 3.91 (s, 2H), 4.12 (s, 1H), 4.59 (d, 1H, *J* = 5.20 Hz), 5.00 (s, 1H), 5.25 (d, 1H, *J* = 5.20 Hz), 6.13 (s, 1H), 8.16 (s, 1H), 8.30 (s, 1H).

*FL-NAH (fluorescein linked with N-adenosylhomocysteine, **6**).* Compound **5** (10 mg, 0.01664 mmol, 1.0 eq.) was dissolved in 3 mL methanol. The compound **1** (15 mg, 0.025 mmol, 1.5 eq.) was added to the solution. Under stirring, sodium ascorbate aqueous solution (0.1664

mmol, 10.0 eq.) was added followed by the aqueous solution of copper (II) sulfate (0.01664 mmol, 1.0 eq.). The mixture was stirred in the darkness at room temperature for 24 h. All liquid was removed by evaporation under strong vacuum. The residue was dissolved in trifluoroacetic acid (TFA, 5 mL) and was stirred in ice bath for 1h. Then double deionized (dd) water (1 mL) was added to the solution. Stirring continued overnight at room temperature. The TFA and water was removed by evaporation and the residue was purified by preparative HPLC to give a yellow color powder (5 mg, 35%). Analytical HPLC purity is 97%. H^+ESI=850.3. ^{1}H-NMR (400MHz, D_2O) δ = 2.16 (m, 1H), 2.38 (m, 1H), 3.35-3.55 (m, 8H), 3.89 (m, 2H), 4.24 (t, 1H, *J* = 4.0 Hz), 4.48-4.60 (m, 3H), 5.97 (s, 1H), 6.54 (d, 2H, *J* = 8.4 Hz), 6.73 (m, 4H), 7.08 (d, 1H, *J* =8.0 Hz), 7.81 (dd, 1H, *J*1 = 8.0 Hz, *J*2 = 1.04 Hz), 8.12 (s, 1H), 8.18 (s, 1H), 8.26 (s, 2H). ^{13}C-NMR (125MHz, D_2O) δ = 172.60, 169.86, 168.15, 162.99, 162.71, 153.88, 150.05, 147.55, 144.88, 142.57, 135.79, 135.19, 132.69, 129.84, 127.98, 126.34, 125.57, 118.84, 117.36, 114.98, 111.19, 102.40, 90.00, 78.27, 73.10, 71.44, 61.61, 54.65, 52.56, 51.72, 49.98, 39.67, 24.67.

Concentration determination of FL-NAH

The FL-NAH purified from HPLC was dissolved in dd-H_2O. Small amount of solution was diluted and adjusted to pH 9 to make sure fluorescein existing as dianion form. The UV absorption was measured at 495 nm. The concentration was calculated with extinction coefficient of 76000 $M^{-1}cm^{-1}$.

Protein expression and purification

Detailed protocols for protein expression and purification can be found in the supplementary information.

Fluorescence polarization assay

All binding experiments were performed in a total volume of 10 µl binding buffer (20 mM Tris pH 8.0 supplemented with 0.01% Triton X-100 and 5 mM DTT) in 384-well black polypropylene PCR plates (Axygen, PCR-384-BK). Fluorescence polarization (FP) was measured using a Biotek Synergy 4 after 30 min incubation at ambient temperature. The excitation and emission wavelength were 485 nm and 528 nm, respectively. Polarization values were expressed in millipolarization units (mP).

Binding of MLL1 to FL-NAH. Increasing concentrations of MLL1 or MLL1 complexes were incubated with 50 nM FL-NAH-1. The binding affinity K_d was calculated by fitting the data to nonlinear least squares regression, single-site binding model using Eq. (1) in GraphPad Prism v. 6.05.

DMSO Tolerance and competitor K_{disp} determination: MLL1 SET domain or complexes were diluted to their respective $K_{d\ (FL\text{-}NAH)}$ concentrations and incubated with 50 nM FL-NAH in the presence of increasing concentrations of DMSO or competitor compounds for 30 minutes at ambient temperature. Fluorescence polarization was measured as described above. The concentration of competitor compound that achieved 50% displacement (K_{disp}) was calculated by fitting the data to nonlinear least squares regression analysis using Eq. (2) in GraphPad Prism v.6.05.

Z' factor analysis. MLL1 SET domain (1 µM) was incubated with 50 nM FL-NAH in the presence or absence of 250 µM SAH. Z' factor was calculated as previously described using Eq. (3)[28].

Equations used for binding evaluations:

The binding affinity K_d was calculated as Eq. (1), where ΔFP is the change of fluorescence polarization, ΔFP_{max} is the maximum ΔFP when MLL1 saturates all the FL-NAH in solution, and [MLL] is the total concentration of the MLL1 SET domain.

$$\Delta FP = \frac{[MLL1]*\Delta FP_{max}}{[MLL1]+K_d} \qquad \textbf{Eq. (1)}$$

The concentration of competitor compound that achieved 50% displacement, $K_{disp,}$ was calculated by Eq. (2), where ΔFP_{bottom} is the lower bound of the concentration-response curve, ΔFP_{top} is the upper bound of the concentration-response curve, [Compound] is the Log of the compound concentration and HS is the Hill Coefficient.

$$\Delta FP = \Delta FP_{bottom} + \frac{(\Delta FP_{top} - \Delta FP_{bottom})}{1+10^{((LogK_{disp}-[Compound])*HS)}} \qquad \textbf{Eq. (2)}$$

Z' factor was calculated as Eq. (3)[28], where σ_N and σ_P are standard deviations for samples without or with SAH, respectively, and μ_N and μ_P are mean FP values for samples in the absence or presence of SAH, respectively.

$$\boldsymbol{Z' = 1 - \frac{(3\sigma_N+3\sigma_P)}{|\mu_N-\mu_P|}} \qquad \textbf{Eq. (3)}$$

ACKNOWLEGEMENTS

The SGC is a registered charity (number 1097737) that receives funds from AbbVie, Bayer Pharma AG, Boehringer Ingelheim, Canada Foundation for Innovation, Eshelman Institute for Innovation, Genome Canada, Innovative Medicines Initiative (EU/EFPIA), Janssen, Merck & Co., Novartis Pharma AG, Ontario Ministry of Economic Development and Innovation, Pfizer, São Paulo Research Foundation-FAPESP, Takeda, and Wellcome Trust. YGZ acknowledges the National Institutes of Health and National Science Foundation for financial supports.

References

1. A. Shilatifard, *Annual review of biochemistry*, 2012, **81**, 65-95.
2. J. H. Lee, C. M. Tate, J. S. You and D. G. Skalnik, *The Journal of biological chemistry*, 2007, **282**, 13419-13428.
3. J. H. Lee and D. G. Skalnik, *The Journal of biological chemistry*, 2005, **280**, 41725-41731.
4. J. Wysocka, T. Swigut, T. A. Milne, Y. Dou, X. Zhang, A. L. Burlingame, R. G. Roeder, A. H. Brivanlou and C. D. Allis, *Cell*, 2005, **121**, 859-872.
5. R. van Nuland, A. H. Smits, P. Pallaki, P. W. Jansen, M. Vermeulen and H. T. Timmers, *Molecular and cellular biology*, 2013, **33**, 2067-2077.
6. S. A. Shinsky, K. E. Monteith, S. Viggiano and M. S. Cosgrove, *The Journal of biological chemistry*, 2015, **290**, 6361-6375.
7. Y. Dou, T. A. Milne, A. J. Ruthenburg, S. Lee, J. W. Lee, G. L. Verdine, C. D. Allis and R. G. Roeder, *Nature structural & molecular biology*, 2006, **13**, 713-719.
8. M. G. Guenther, R. G. Jenner, B. Chevalier, T. Nakamura, C. M. Croce, E. Canaani and R. A. Young, *Proceedings of the National Academy of Sciences of the United States of America*, 2005, **102**, 8603-8608.
9. C. W. Chen and S. A. Armstrong, *Experimental hematology*, 2015, DOI: 10.1016/j.exphem.2015.05.012.
10. R. L. Wright and A. T. Vaughan, *Critical reviews in oncology/hematology*, 2014, DOI: 10.1016/j.critrevonc.2014.03.004.
11. A. Shi, M. J. Murai, S. He, G. Lund, T. Hartley, T. Purohit, G. Reddy, M. Chruszcz, J. Grembecka and T. Cierpicki, *Blood*, 2012, **120**, 4461-4469.
12. J. Manka, R. N. Daniels, E. Dawson, J. S. Daniels, N. Southall, A. Jadhav, W. Zheng, C. Austin, J. Grembecka, T. Cierpicki, C. W. Lindsley and S. R. Stauffer, in *Probe Reports from the NIH Molecular Libraries Program*, Bethesda (MD), 2010.
13. L. Li, R. Zhou, H. Geng, L. Yue, F. Ye, Y. Xie, J. Liu, X. Kong, H. Jiang, J. Huang and C. Luo, *Bioorganic & medicinal chemistry letters*, 2014, **24**, 2090-2093.
14. S. He, T. J. Senter, J. Pollock, C. Han, S. K. Upadhyay, T. Purohit, R. D. Gogliotti, C. W. Lindsley, T. Cierpicki, S. R. Stauffer and J. Grembecka, *Journal of medicinal chemistry*, 2014, **57**, 1543-1556.
15. J. Grembecka, S. He, A. Shi, T. Purohit, A. G. Muntean, R. J. Sorenson, H. D. Showalter, M. J. Murai, A. M. Belcher, T. Hartley, J. L. Hess and T. Cierpicki, *Nature chemical biology*, 2012, **8**, 277-284.
16. A. T. Thiel, P. Blessington, T. Zou, D. Feather, X. Wu, J. Yan, H. Zhang, Z. Liu, P. Ernst, G. A. Koretzky and X. Hua, *Cancer cell*, 2010, **17**, 148-159.
17. G. Senisterra, H. Wu, A. Allali-Hassani, G. A. Wasney, D. Barsyte-Lovejoy, L. Dombrovski, A. Dong, K. T. Nguyen, D. Smil, Y. Bolshan, T. Hajian, H. He, A. Seitova, I. Chau, F. Li, G. Poda, J. F. Couture, P. J. Brown, R. Al-Awar, M. Schapira, C. H. Arrowsmith and M. Vedadi, *The Biochemical journal*, 2013, **449**, 151-159.
18. F. Cao, E. C. Townsend, H. Karatas, J. Xu, L. Li, S. Lee, L. Liu, Y. Chen, P. Ouillette, J. Zhu, J. L. Hess, P. Atadja, M. Lei, Z. S. Qin, S. Malek, S. Wang and Y. Dou, *Molecular cell*, 2014, **53**, 247-261.
19. T. Cierpicki and J. Grembecka, *Future medicinal chemistry*, 2014, **6**, 447-462.

20. M. V. Florian Grebien, Matthäus Getlik, Roberto Giambruno, Amit Grover, Roberto Avellino, Anna Skucha, Sarah Vittori, Ekaterina Kuznetsova, David Smil, Dalia Barsyte-Lovejoy, Fengling Li, Gennadiy Poda, Matthieu Schapira, Hong Wu, Aiping Dong, Guillermo Senisterra, Alexey Stukalov, Kilian V. M. Huber, Andreas Schönegger, Richard Marcellus, Martin Bilban, Christoph Bock, Peter J. Brown, Johannes Zuber, Keiryn L. Bennett, Rima Al-awar, Ruud Delwel, Claus Nerlov, Cheryl H. Arrowsmith and Giulio Superti-Furga *Nature chemical biology*, 2015.
21. L. J. Brown, M. Baranowski, Y. Wang, A. K. Schrey, T. Lenz, S. D. Taverna, P. A. Cole and M. Sefkow, *Analytical biochemistry*, 2014, **467**, 14-21.
22. J. S. Yi, A. J. Federation, J. Qi, S. Dhe-Paganon, M. Hadler, X. Xu, R. St Pierre, A. C. Varca, L. Wu, J. J. Marineau, W. B. Smith, A. Souza, E. J. Chory, S. A. Armstrong and J. E. Bradner, *ACS chemical biology*, 2015, **10**, 667-674.
23. S. D. Barrett, D. A. Bochar, L. L. Blazer, F. L. Ciske, G. W. Endres, J. K. Johnson, G. S. Keyes, R. S. Sidhu, R. C. Trievel and M. L. Collins, *USPTO, US 2012/0295283 A1*, 2012.
24. J. Dowden, W. Hong, R. V. Parry, R. A. Pike and S. G. Ward, *Bioorganic & medicinal chemistry letters*, 2010, **20**, 2103-2105.
25. G. Zhang, S. L. Richardson, Y. Mao and R. Huang, *Organic & biomolecular chemistry*, 2015, **13**, 4149-4154.
26. S. M. Southall, P. S. Wong, Z. Odho, S. M. Roe and J. R. Wilson, *Molecular cell*, 2009, **33**, 181-191.
27. P. Wanat, S. Walczak, B. A. Wojtczak, M. Nowakowska, J. Jemielity and J. Kowalska, *Organic letters*, 2015, **17**, 3062-3065.
28. J. H. Zhang, T. D. Chung and K. R. Oldenburg, *Journal of biomolecular screening*, 1999, **4**, 67-73.

Tables

Table 1. Binding affinities and ΔFP_{max} of FL-NAH binding to MLL1 SET domain. Isolated MLL1 SET domain (SET Only) or in the context of various complexes were allowed to bind to FL-NAH as described in *Materials and Methods*. Saturation data were fitted using non-linear least squares regression analysis. Data are presented as the mean ± SD from at least three independent experiments.

Complex	K_d (μM)	ΔFP_{max}
SET Only	1 ± 0.1	240 ± 3
Trimeric	7 ± 3	260 ± 40
Tetrameric	1.4 ± 0.4	300 ± 30
Pentameric	0.2 ± 0.03	270 ± 20

Table 2. Displacement of FL-NAH from the MLL1 SAM-binding site. Displacement of FL-NAH from the SAM-binding site of isolated MLL1 SET domain or in various MLL1 complexes by SAH, SAM or sinefungin was measured as described in material and methods. Data are presented as the mean ± SD from at least three independent experiments.

	SAH		SAM		Sinefungin	
Complex	**K_{disp} (μM)**	**Hill Slope**	**K_{disp} (μM)**	**Hill Slope**	**K_{disp} (μM)**	**Hill Slope**
SET Only	4 ± 0.5	-0.9 ± 0.2	14 ± 2	-1.2 ± 0.1	9 ± 0.2	-0.9 ± 0.1
Trimeric	2 ± 0.2	-1.5 ± 0.3	7 ± 1	-1.6 ± 0.4	10 ± 2.5	-1.1 ± 0.3
Tetrameric	0.3 ± 0.1	-1.9 ± 0.1	1 ± 0.1	-1.7 ± 0.2	2 ± 0.2	-1.2 ± 0.1
Pentameric	0.2 ± 0.02	-1.4 ± 0.3	1 ± 0.2	-1.6 ± 0.3	0.5 ± 0.1	-1.1 ± 0.3

Figure legends

Scheme 1. Synthesis of FL-NAH. a. HOBt, EDCI, TEA, DMF; b. DPPA, DBU, NaN3, 15-crown-5, under nitrogen, 1,4-dioxane; c. hydrogen, Pd/C in MeOH; d. $Na(AcO)_3BH$, DCE; e. propargyl bromide, K_2CO_3, DMF, r.t.; f. $CuSO_4$, sodium ascorbate, H_2O and MeOH; g. TFA and water

Figure 1. Chemical structure of the fluorescent probe FL-NAH.

Figure 2. Saturation of the isolated MLL1 SET domain with FL-NAH. The isolated SET domain of MLL1 binds to FL-NAH with an affinity of 1 ± 0.1 μM. FL-NAH (50 nM) was incubated with increasing concentrations of MLL1 SET domain. Fluorescence polarization was measured after 30 minutes incubation. Data are presented as the mean ± SD from three independent experiments.

Figure 3. Displacement of FL-NAH by various compounds. FL-NAH is displaced from the isolated SET domain by A) SAM with a K_{disp} of 14 ± 2 μM, B) SAH with a K_{disp} of 4 ± 0.5 μM, C) Sinefungin with a K_{disp} of 9 ± 0.2 μM, but is not by D) the substrate peptide H3 (1-25). Data are presented as the mean ± SD from three independent experiments.

Figure 4. FL-NAH displacement assay in a 384-well format. A) FL-NAH binding to MLL1 is stable in the presence of at least 10% DMSO. Data are presented as the mean ± SD from three independent experiments. B) The optimized 384-well format provides a Z' of 0.7 when 250 μM SAH is used as a positive control. Data are presented from 192 wells each of positive (Δ; 250

μM SAH) and negative (■; vehicle) controls. Dashed lines represent ± 3 standard deviations from the mean value of each control.

Scheme 1. Synthesis of FL-NAH.

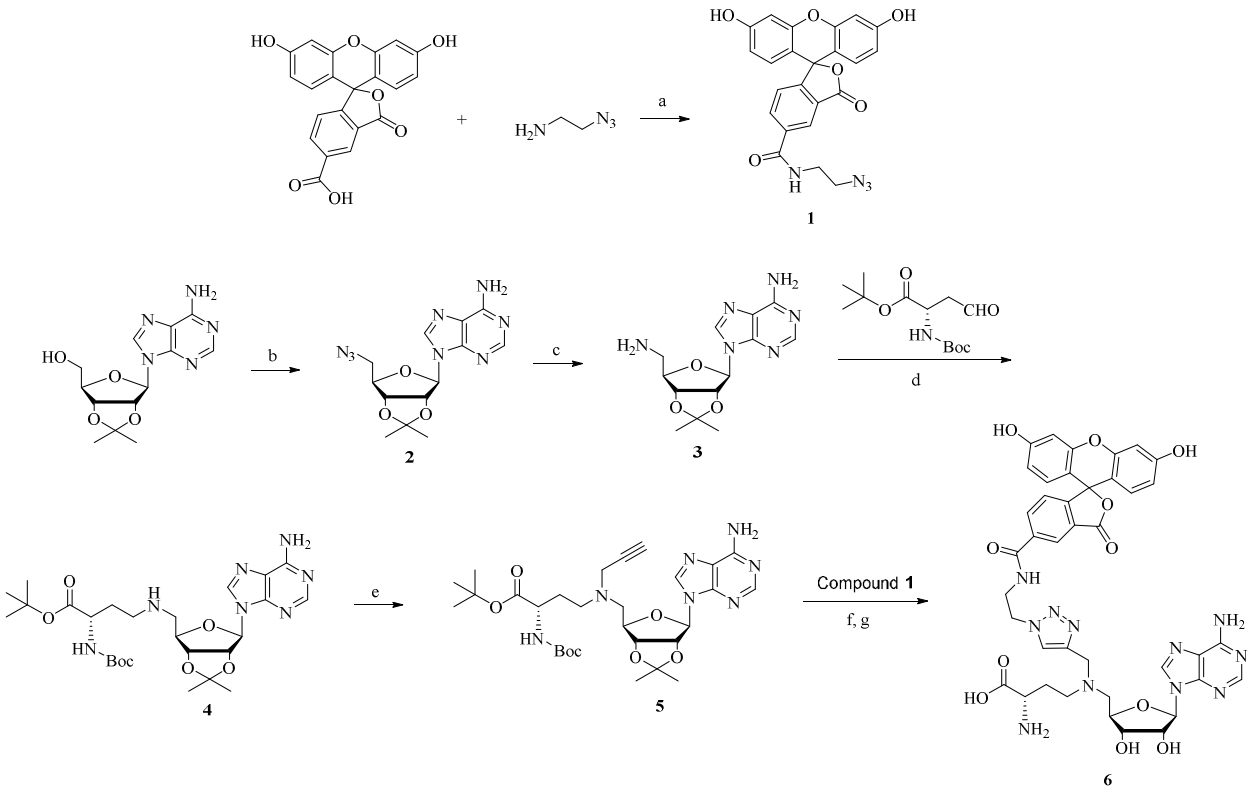

Figure 1

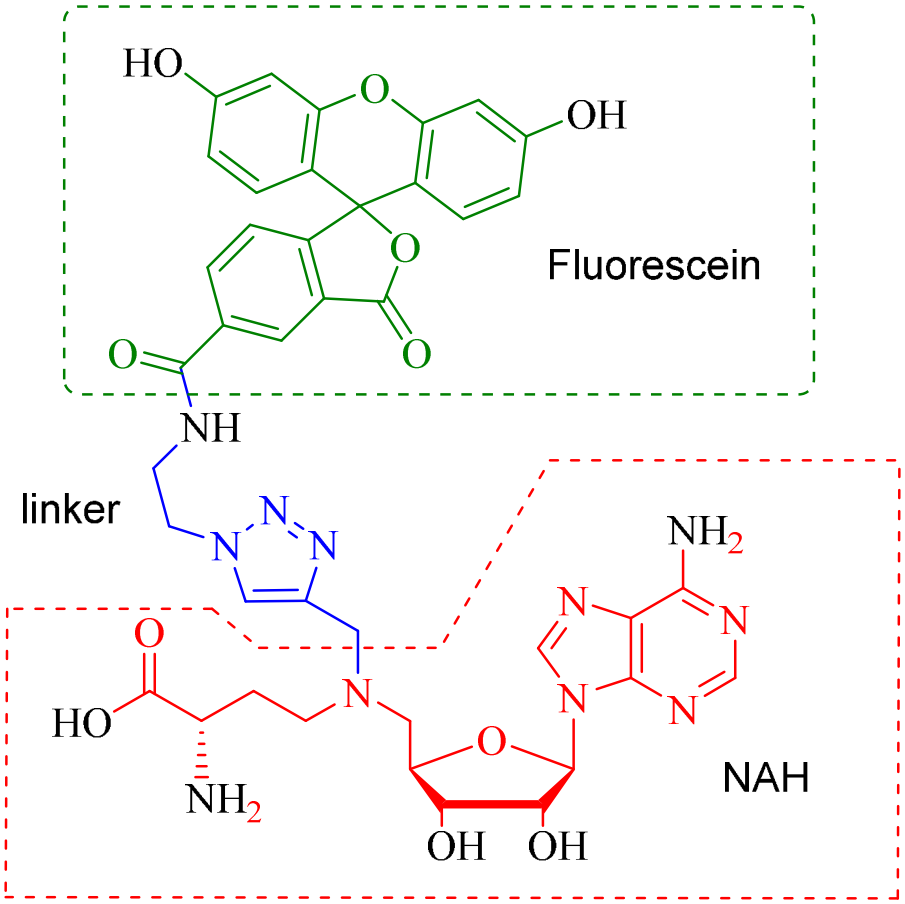

Figure 2

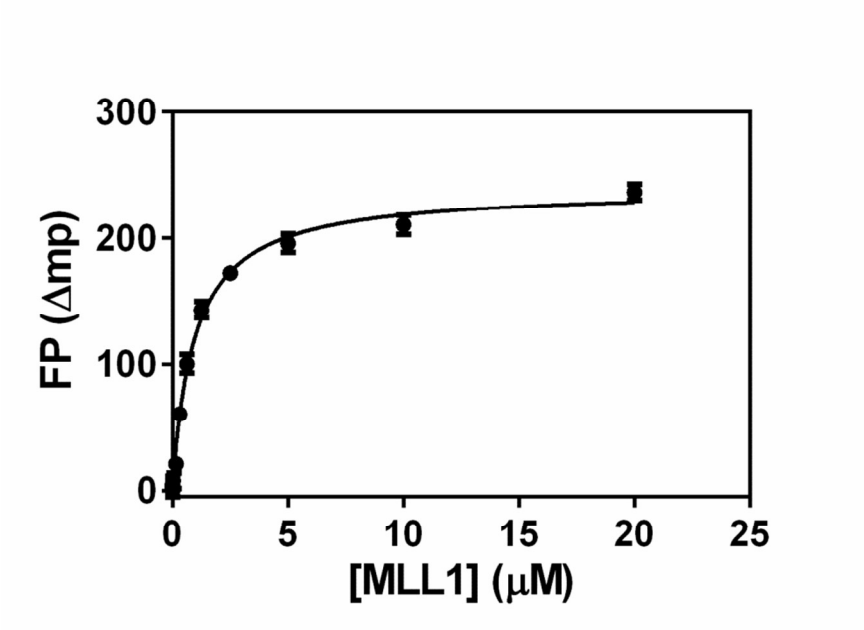

Figure 3

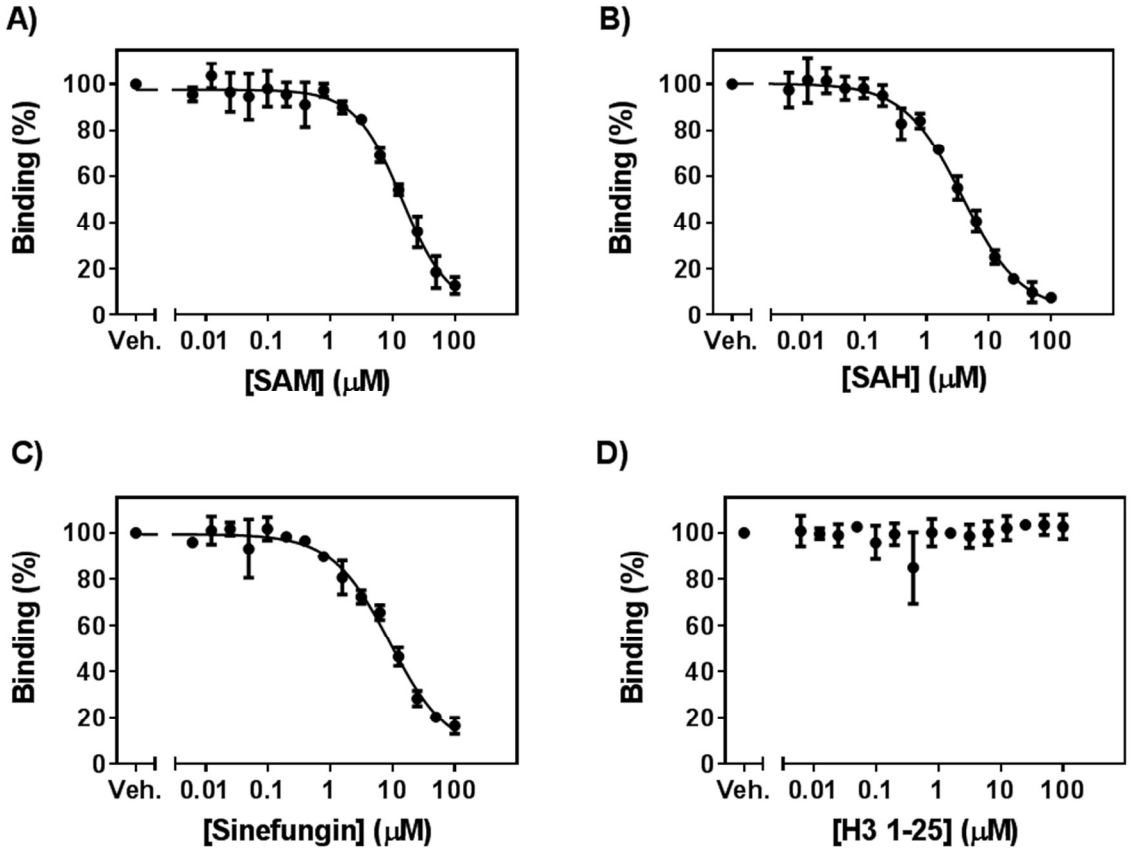

Figure 4